COMSOL Assistance for the Determination of Pressure Drops in Complex Microfluidic Channels

J. Berthier*, R. Renaudot , P. Dalle, G. Blanco-Gomez, F. Rivera, V. Agache and P. Caillat.
CEA-LETI-Minatec, Department of Biotechnology
*Corresponding author: CEA, 17 avenue des Martyrs, 38054, Grenoble, France, jean.berthier@cea.fr

Abstract:

With the current trend towards always more complexity associated to more functionalities in biotechnological systems, it is required to know with accuracy the pressure drop in the circuitry of microfluidic systems. In general, a full three-dimensional calculation is not tractable due to the limited capacity of the computers. However, computational models can help to produce pressure drop correlations. In this work, we use COMSOL to contribute to the determination of pressure drops in different types of geometry, typical of biochips, like rectangular and pillared channels, and for different liquids, including non-Newtonian biologic liquids. We show that the numerical results agree with the theoretical results—when they exist—and investigate the potentialities and limits of the 2D-Helle-Shaw formulation.

Keywords: Pressure-drop, posted arrays, pillar, non-Newtonian fluid

1. Introduction

In this work, the laminar pressure drops in microchannels have been investigated for three cases: first, in rectangular channels for which analytical approximate solutions exist [1,2,3]. It is shown here that the 3D-COMSOL numerical results reproduce quite well the pressure drop obtained by analytical models. On the other hand, the 2D-Helle-Shaw (noted 2D-HS) formulation is accurate under the condition that the channel depth d is small compared to its width w [2,3]. Indeed, the 2D-HS formulation

$$\rho\left(\vec{U}.\nabla\right)\vec{U} = -\nabla P + \mu\,\Delta\vec{U} - 12\,\mu/d^2\,\vec{U}\,, \qquad (1)$$

where ρ and μ are respectively the density and visocity of the fluid, supposes a vertical parabolic profile, which is exact for an aspect ratio smaller than 1/3. In (1), P is the pressure, U the velocity, ρ the liquid density and μ the liquid viscosity. Second, we investigate the pressure drop in pillared channels. We indicate the domain where the 2D-HS is accurate and derive a scaling law in this domain. Finally, we investigate the case of non-Newtonian liquids flowing in cylindrical and rectangular channels. The COMSOL results agree with the Rabinowitsch-Mooney model for a cylindrical duct and with Kozicki and Muzyckha models for rectangular channels [4,5]. A simplified expression is deduced from the COMSOL approach for square channels..

2. Pressure drop in rectangular channels

Flow channels in microsystems are usually rectangular. This is due to the microfabrication process. Pressure drops in such channels have been largely documented [1,2,3]. The most used formula to calculate the laminar pressure drop in a rectangular microchannel of aspect ratio $\varepsilon = \min(w/d, d/w)$—where d and w are the two dimensions of the cross section—is the expression [2,3]

$$\Delta P = R\,Q\,, \qquad (2)$$

with

$$R = 4\,\mu\,L\,/\left(w\,d\,\min(w^2, d^2)\,q(\varepsilon)\right),$$

where the function q is the form factor given by

$$q(\varepsilon) = 1/3 - \left(64/\pi^5\right)\varepsilon\,\tanh\left(\pi/2\,\varepsilon\right).$$

A good agreement with the theoretical formula is obtained by a 3D calculation with COMSOL. A good agreement is also obtained by using a 2D Helle-Shaw calculation when the aspect ratio is less than 1/3 [1,2]. For larger aspect ratios (1/3 to 1) the agreement is a little less satisfactory, but this method still yields an approximation of the pressure drop (fig.1). In a typical case of a channel of width w=100 µm, length L=400 µm and flow rate Q=1 µl/mn, the analytical and 3D-COMSOL

pressure profiles are nearly indiscernible for any aspect ratio, whereas the 2D-HS model is adequate for aspect ratios less than 1/3 approximately: relative errors of 2°/$_{oo}$, 3% and 5% are respectively found for aspect ratios of 2/5, ½ and 1. Note that the pressure drop is much larger for a small aspect ratio channel under the same flow rate conditions.

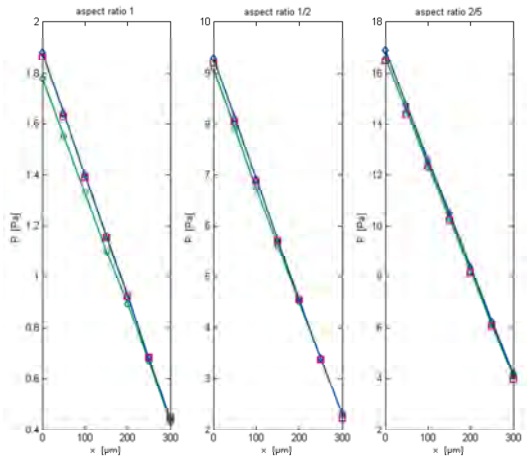

Figure 1. Comparison of the pressure profile in a rectangular channel between analytical expression (red squares), 3D-COMSOL (continuous blue line with diamonds) and 2D-HS-COMSOL (continuous green line with circles) formulations, for three different aspect ratios:

3. Pressure drop in pillared channel

Pillared channels are commonly used in microfluidic systems. Pillars have two main functions: first, they can be used as additional active surface for performing heterogeneous wall biochemical reactions [6]; they provide a large surface over volume ratio that promotes the contact or capture of targets on the functionalized pillars. The second use of pillars (or posts) is mechanical: micropillars (even nano-pillars) are used to facilitate the direct bonding process of the cover plate that seals the microsystem; this is especially the case of extremely small channels, at the limit of the nanoscales. In such a case, micro-pillar tops bring additional contact for the cover plate and limit the "free" suspended area [7,8] (fig.2).

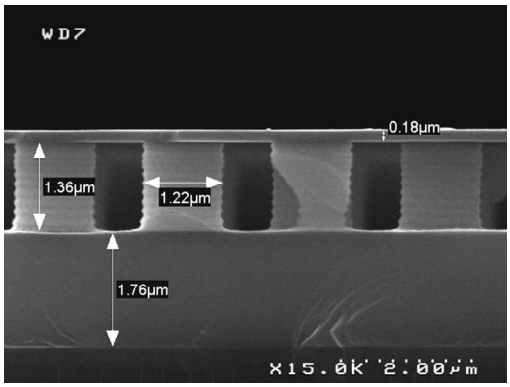

Fig.2. SEM image of the cross- section of a pillared microchannel, showing the thin cover plate sealing the microsystem [7] (photo courtesy V. Agache).

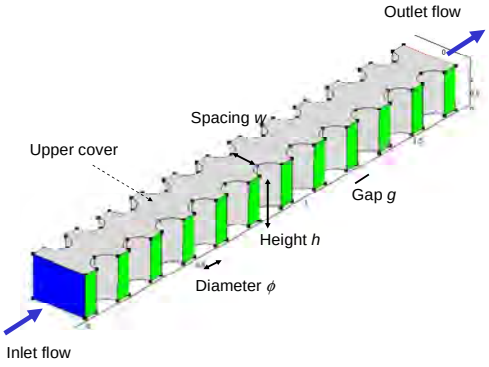

Fig.3. Model for the flow calculation in a slice of pillared channel.

Many parameters are associated with a pillared geometry: pillar height (h), gaps (g along the flow direction and w perpendicular to it), the pillar diameter ϕ, the length L and width W of the outer boundaries (fig.3). Let us assume that the global scales W and L are much larger than the local scales w and g. In a recent publication, Srivastava et al. have numerically investigated with COMSOL the case where the spacing is homogeneous—i.e. $w=g$ and the aspect ratio h/w larger than 1 [9]. In this work we focus on smaller aspect ratios $h/w \in [0.1,1]$, and we take into account non homogeneous spacing, i.e. $w \neq g$.

The numerical approach is straightforward: the Navier-Stokes equation is used with the standard boundary conditions (specified inlet velocities and zero pressure at the outlet). The mesh number is

the largest possible taken into account the computer memory, and the convergence of the solution with the mesh size has been checked.

First, it is numerically observed that, in the parametric domain defined by

$$\Omega = \left\{ \begin{array}{c} h/w \le 1 \\ 0.5 \le g/w \le 2 \\ 0.5 < w/\phi < 2 \\ w << W \\ g << L \end{array} \right\},$$

and shown in figure 4, the 2D-HS model developed for rectangular cross section is valid. It implicitly means that the vertical velocity profile is approximately quadratic, even when the axial flow is modified by the presence of pillars. Besides, in the domain Ω, the COMSOL approach leads to the relation

$$\frac{\partial P}{\partial x} \approx \frac{130\ \mu\ Q\ \phi^{0.1}}{h^2\ w^2\ g^{0.1}} \qquad (3)$$

Figures 5, 6 and 7 show the variation of $\partial P/\partial x$ respectively with $1/h^2$, $1/w^2$ and $1/g^{0.1}$. Note that W and L do not appear in (3) because they are assumed to be much larger than w and g. Note also that it is not needed to investigate the variation of $\partial P/\partial x$ with ϕ—which would be very lengthy—because the exponent of ϕ is directly obtained by a dimensional analysis of (3).

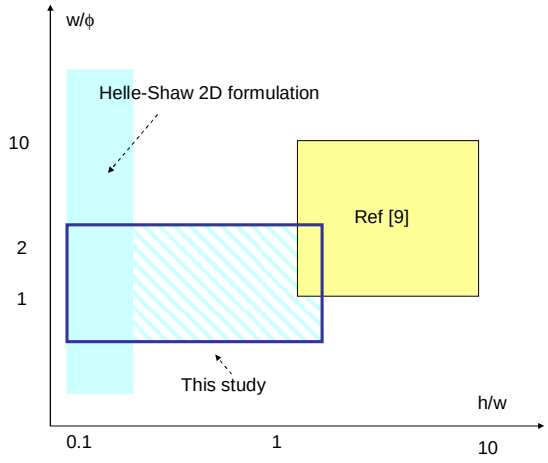

Fig.4. Domain of validity of the present work and [9].

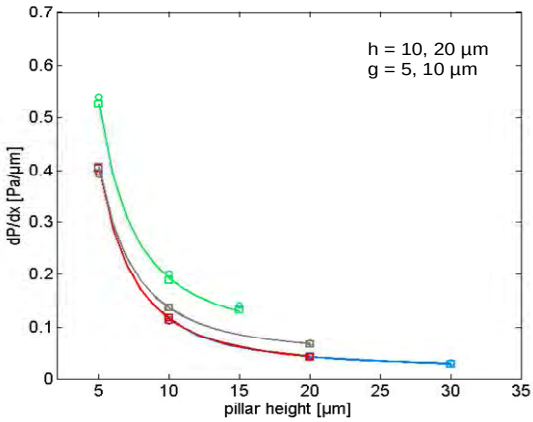

Fig.5. Pressure gradient as a function of the height of the channel h: the dots correspond to COMSOL (3D and HS) calculations and the continuous line to the power law $1/h^2$. Note that the HS formulation is very close to the full 3D model.

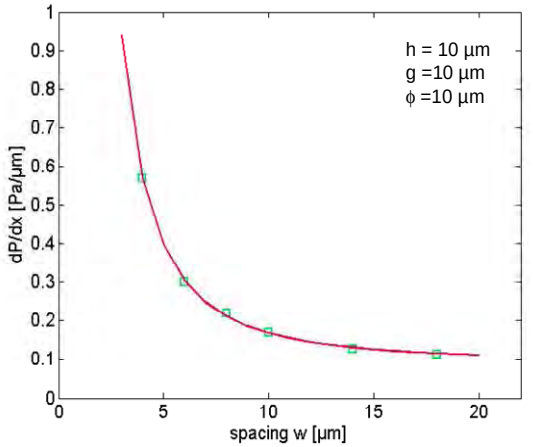

Fig.6. Pressure gradient as a function of the axial spacing w: the dots correspond to COMSOL (3D and HS) calculations and the continuous line to the power law $1/w^2$.

In conclusion, for aspect ratios smaller than 1, the Helle-Shaw model (1) correctly predicts the pressure drop in the domain Ω. Moreover, relation (3) is fast and convenient for the prediction of the pressure drop in Ω.

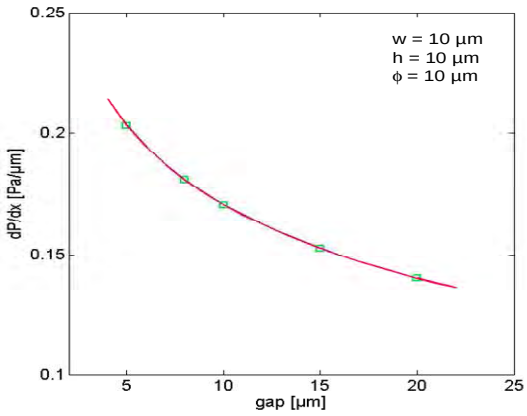

Fig.7. Pressure gradient as a function of the gap: dots correspond to COMSOL (3D and HS) calculations and the continuous line to the power law $1/g^{0.1}$.

4. Pressure drop of non-Newtonian liquids in microchannels

In modern biotechnology, viscoelastic fluids like whole blood or alginates, xanthan, etc. are increasingly used. This is for example the case of cell encapsulation in alginates (Fig.8). However, pressure drop determination of non-Newtonian fluid flows remains a challenge. Indeed, for a Newtonian fluid, the force balance on a control volume of a rectangular channel of width *w*, depth *d* and wall surface *S*, can be expressed as

$$\Delta P = \frac{1}{w\,d}\int_S \tau_w \, ds \qquad (4)$$

where τ_w is the wall friction. For a 2D case, and a Poiseuille flow, the wall friction is simply given by

$$\tau_w = \frac{6\mu\overline{U}}{d} \qquad (5)$$

where μ is the viscosity and $\overline{U}$ the average velocity. Substitution of (5) in (4) yields

$$\Delta P = \frac{12\,\mu L\overline{U}}{d^2} \qquad (6)$$

where *L* is the length of the control volume.

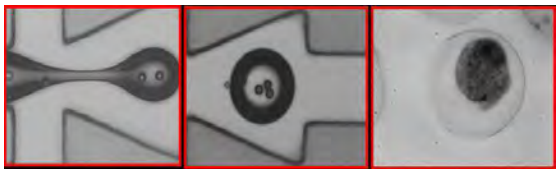

Fig.8. Encapsulation of cells in visco-elastic alginates (photo courtesy P. Dalle).

However, in the case of a non-Newtonian fluid, equation (4) becomes a complicated integral

$$\Delta P = \frac{1}{w\,d}\int_S \eta\left(\dot{\gamma}_w\right)\,\dot{\gamma}_w \, dx\,dy\,dz \qquad (7)$$

where $\dot{\gamma}_w$ is the wall shear rate. The only case for which a closed form formulation exists is that of a cylindrical duct in which a 'power law' fluid (Ostwald fluid) circulates. It is recalled that the viscosity of a 'power law' fluid has the form

$$\eta = K\,\dot{\gamma}^{n-1} \qquad (8)$$

where *K* and *n* are constants, and the friction is expressed by

$$\tau = \eta\,\dot{\gamma} = K\,\dot{\gamma}^{n} \qquad (9)$$

Note that, even if the fluid is not exactly an Ostwald fluid, its viscosity can often be approximated by a power law. For example, in the case of alginates—widely used in biotechnology and biology—it has been shown that they obey a Carreau-Yasuda relation [10]. A power law approximation can be found by setting *K*=0.5 and *n*=0.8 (Fig.9).

In such a case, the solution has been formally given by Rabinowitsch and Mooney [4]

$$\Delta P_{RM} = \frac{2^{(n+2)}\,L\,K}{w}\left(\frac{3n+1}{n}\right)^n\left(\frac{\overline{U}}{w}\right)^n \qquad (10)$$

where *K* and *n* are the constant of the 'power law' fluid. Hence, the hydraulic resistance is

$$R_{RM} = \frac{2^{(n+2)}\,L\,K}{w^3\,d}\left(\frac{3n+1}{n}\right)^n\left(\frac{\overline{U}}{w}\right)^{n-1} \qquad (11)$$

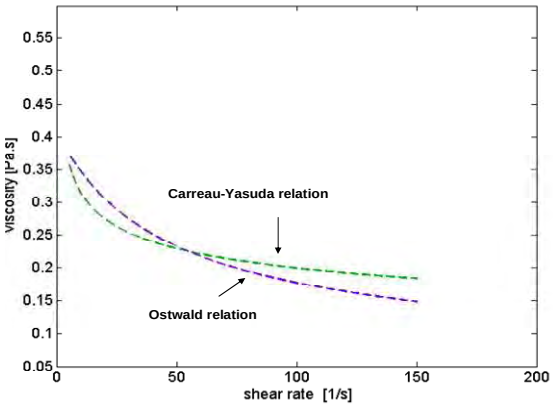

Fig.9. Comparison between the nearly exact Carreau-Yasuda relation for the viscosity and a simple power law (Ostawald relation).

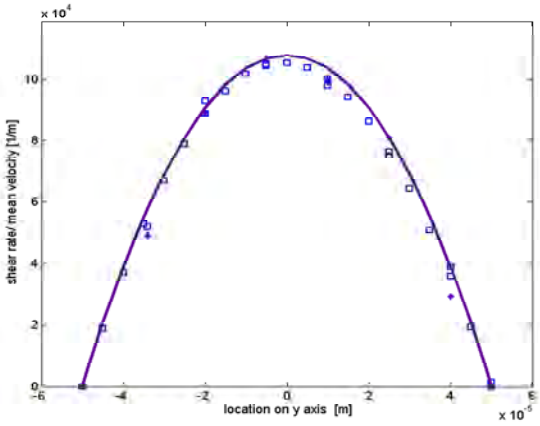

Fig.10. Reduced wall shear rates obtained using COMSOL and second order polynomial fit.

Relation (11) shows that the hydraulic resistance is not a geometrical constant, and depends on the flow velocity. This is a drastic difference between Newtonian and non-Newtonian fluids that has important consequences on microfluidic networks [11]. Inspired by the cylindrical approach, approximated relations have been found for rectangular channels [5,12-14], leading to the expression

$$\Delta P = \frac{2^{3n+2}\, K\, L}{w^{n+1}} \left(\frac{c_1}{n} + c_2 \right)^n \overline{U}^n \qquad (12)$$

where the geometric coefficient c_1 and c_2 are given in appendix 1. The hydraulic resistance of a rectangular channel is then

$$R = \frac{2^{3n+2}\, K\, L}{w^3\, d} \left(\frac{c_1}{n} + c_2 \right)^n \left(\frac{\overline{U}}{w} \right)^{n-1}. \qquad (13)$$

Again, it is observed that the hydraulic resistance depends on the flow conditions.

We have numerically investigated the case of a square channel using different power law—varying K and n in (8)—and different flow rates with the COMSOL numerical software. It appears that the wall friction collapses in all the considered cases on the same quadratic law, even if the velocity profile is not quadratic in the central part of the channel (Fig.10). The wall shear rate is given by the relation

$$\dot{\gamma}(y) = 1.2\, \overline{U} \left[\frac{k+1}{k} \right]^2 \frac{k}{a} \left[1 - \left(\frac{y}{a} \right)^k \right]. \qquad (14)$$

where k =2. Hence, the pressure drop is then given by the relation

$$\Delta P = \frac{4\, L\, K}{w} \left[10.8\, \frac{\overline{U}}{w} \right]^n \int_0^{\pi/2} \sin^{2n+1}\theta \, d\theta \qquad (15)$$

The advantage of this latter formulation over (12) is that no geometrical coefficient is needed. The hydraulic resistance can be cast under the form

$$R = \frac{4\, L\, K}{w^3\, d} \left[10.8\, \frac{\overline{U}}{w} \right]^{n-1} \int_0^{\pi/2} \sin^{2n+1}\theta \, d\theta \qquad (16)$$

Figure 11 shows a comparison between the literature results (Kozicki et al. Muzychka et al. and Miller), correlation (14) deduced from COMSOL calculations and COMSOL 3D calculation for a 100 µm channel.

5. Conclusion

If the aspect ratio of a rectangular micro-channel is small enough, the 2D-Helle-Shaw approach is valid. It is less accurate for aspect ratios slightly above 1.

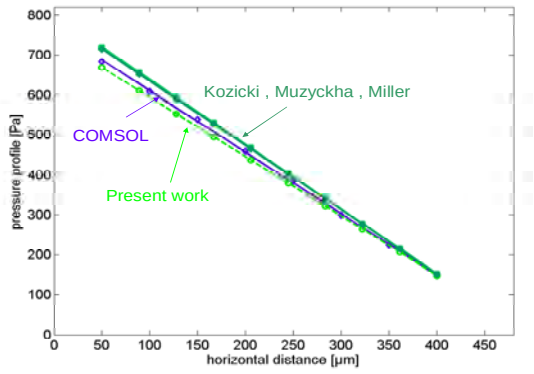

Fig.10. Non-Newtonian pressure profiles in a 100 µm x 100 µm square channel of length L= 500 µm.

It is also valid for pillared channels of relatively small aspect ratios. Using a similar numerical approach as that of [9], a scaling law for the pressure drop has been derived. This scaling law, valid for small aspect ratios, differs considerably from that of [9], valid for high aspect ratios. A universal law is still to be found.

Non-Newtonian flows are complex and only the case of Ostwald fluids in cylindrical or rectangular channels has been investigated in the literature. The COMSOL numerical approach agrees with the published results, and has been used to derive a pressure drop correlation for a square channel, requiring no geometrical coefficients.

6. References

1. M. Bahrami, M. M. Yovanovich, J. R. Culham, Pressure drop of fully-developed, laminar flow in microchannels of arbitrary cross section, *Proceedings of ICMM 2005*, 3rd International Conference on Microchannels and Minichannels, June 13-15, 2005, Toronto, Ontario, Canada, 2005.
2. H. Bruus. *Theoretical microfluidics*. Oxford Master Series in Condensed Matter Physics, 2008.
3. J. Berthier, P. Silberzan. *Microfluidics for Biotechnology*. Second Edition, Artech House, 2010.
4. J.F. Steffe. *Rheological methods in food process engineering*. Second Edition, Freeman Press, 1982.
5. Y.S. Muzychka, J.F. Edge, Laminar non-Newtonian fluid flow in non-circular ducts and microchannels, *J. Fluid Engineering*, **130**, n°11, p. 111-201, 2008.
6. S.R.A. de Loos, J. van der Schaaf, M.H.J.M. de Croon, T.A. Nijhuis, R.M. Tiggelaar, H.G.E. Gardeniers and J.C. Schouten, Three-Phase Mass Transfer in Pillared Micro Channels, *Proceedings of the 10th International Conference on Microreaction Technology, IMRET 2008*, New Orleans, 1-4 April, 2008.
7. V. Agache, Dispositif pour la détection gravimétrique de particules en milieu fluide, comprenant un oscillateur traversé par une veine fluidique, procédé de réalisation et méthode de mise en œuvre du dispositif, International patent WO/2009/141516– 26/11/2009.
8. Pyung-Soo Lee, Junghyun Lee, Nayoung Shin, Kun-Hong Lee, Dongkyu Lee, Sangmin Jeon, Dukhyun Choi, Woonbong Hwang, and Hyunchul Park. Microcantilevers with Nanochannels. *Adv. Mater*. 2008, **20**, 1732–1737.
9. N. Srivastava, C. Din, A. Judson, N.C. MacDonald, C.D. Meinhart, A unified scaling model for flow through a lattice of microfabricated posts, *Lab Chip*, **10**, 1148-1152, 2010.
10. J. Berthier, S. Le Vot, P. Tiquet, N. David, D. Lauro, P.Y. Benhamou, F. Rivera. Highly viscous fluids in pressure actuated flow focusing devices, *Sensors and Actuators* A **158** (2010) 140–148.
11. J. Berthier, S. Le Vot, P. Tiquet, F. Rivera, P. Caillat, On the influence of non-Newtonian fluids on microsystems for biotechnology. *Proceedings of the 2009 Nanotech-NSTI Conference*, 3-7 May 2009, Houston, USA.
12. W. Kosicki, C.H. Chou, C. Tiu, Non-Newtonian Flow in Ducts of Arbitrary Cross-sectional Shape, *Chemical Engineering Science*, **21** (1966), pp. 665–679.
13. C. Miller, Predicting non-Newtonian flow behaviour in ducts of unusual cross section, *Ind. Eng. Chem. Fundam.* **11** (1972), pp. 534–628.
14. F. Delplace, J.C. Leuliet, Generalized Reynolds number for the flow of power law fluids in cylindrical ducts of arbitrary cross-section. *Chem.Eng. Journal*,.**56**, (1995),pp.33-37.

Appendix 1: Kozicki expression for the pressure drop.

First, a non-dimensional friction is defined by

$$\tau^*_{wall,\sqrt{A}} = 2^n \left(\frac{c_1}{n} + c_2\right)^n \left(\frac{2(\varepsilon+1)}{\sqrt{\varepsilon}}\right)^n, \quad \text{(A.1)}$$

where $\varepsilon = min(w/d, d/w)$ is the aspect ratio. It is recalled that for square channels ε=1. The geometrical constant c_1 and c_2 are then

$$c_1 = \frac{1}{2(1+\varepsilon)^2\left(1 - \frac{32}{\pi^3 \cosh\left(\frac{\pi}{2\varepsilon}\right)}\right)} \quad \text{(A.2)}$$

$$c_2 = \frac{3}{2(1+\varepsilon)^2\left(1 - \frac{192\varepsilon \tanh\left(\frac{\pi}{2\varepsilon}\right)}{\pi^5}\right)} - c_1$$

Then, the dimensional friction is

$$\tau_{wall,\sqrt{A}} = \frac{\tau^*_{wall,\sqrt{A}}\, K U^n}{\left(\sqrt{A}\right)^n} = 2^n \left(\frac{c_1}{n} + c_2\right)^n \left(\frac{2(\varepsilon+1)}{\sqrt{\varepsilon}}\right)^n \frac{K U^n}{\left(\sqrt{A}\right)^n} \quad \text{(A.3)}$$

Finally the pressure drop is

$$\Delta P \frac{2^{3n+2} K L}{w^{n+1}} \left(\frac{c_1}{n} + c_2\right)^n U^n \quad \text{(A.4)}$$